Rare Metal Materials and Engineering
Volume 52, Issue 3, March 2023
Available online at www.rmme.ac.cn

Science Press

Cite this article as: Wang Lingjiao, Li Xiaoqiang, Pan Cunliang, et al. Effect of Nonisothermal Creep Aging on Mechanical Properties and Corrosion Resistance of Al-Zn-Mg-Cu Alloy[J]. Rare Metal Materials and Engineering, 2023, 52(03): 867-875.

ARTICLE

Effect of Nonisothermal Creep Aging on Mechanical Properties and Corrosion Resistance of Al-Zn-Mg-Cu Alloy

Wang Lingjiao[1,2], Li Xiaoqiang[1,2], Pan Cunliang[1,2], Zhu Dezhi[1,2], Qu Shengguan[1,2], Huang Xia[3]

[1] Guangdong Key Laboratory for Advanced Metallic Materials Fabrication and Forming, South China University of Technology, Guangzhou 510640, China; [2] National Engineering Research Center of Near-Net-Shape Forming for Metallic Materials, South China University of Technology, Guangzhou 510640, China; [3] AVIC Manufacturing Technology Institute, Beijing 100024, China

Abstract: The effects of the heating rate and peak temperature on the springback, mechanical properties, and corrosion resistance of Al-Zn-Mg-Cu alloy were investigated. The precipitation behavior and aging strengthening mechanism of the alloy were analyzed by transmission electron microscope. Results show that with decreasing the heating rate and increasing the peak temperature, the springback of the alloy is decreased; the size of intragranular precipitates is increased; the volume fraction of intragranular precipitates is firstly increased and then decreased; the grain boundary precipitates become discontinuous and the precipitate-free zone is expanded. After nonisothermal creep aging (NICA) treatment (20 °C/h, 180 °C), the main precipitates of alloy are compact η' phase, the grain boundary precipitates are discontinuous, and the free zone width is approximately 44.2 nm. The mechanical properties and corrosion resistance of the alloy treated by NICA (20 °C/h, 180 °C) are better than those of the alloy treated by common isothermal creep aging (120 °C, 24 h), and the aging time is shortened by 67%.

Key words: Al-Zn-Mg-Cu alloy; nonisothermal creep aging; precipitation phase; mechanical properties; corrosion resistance

Al-Zn-Mg-Cu alloys are commonly used in the aerospace industry due to their high strength[1–2]. The components produced by the traditional process, such as shape forming followed by aging hardening, often have residual stress[3]. Therefore, the creep age forming (CAF) method is proposed, which is an efficient metal forming way to manufacture the large-scale integral aluminum alloy structures with low residual stress. The high pressure or mechanical clamping is adopted to load the plate on the mold and then the alloy is treated by appropriate artificial aging process. Under the action of thermal-mechanical fields, partial elastic deformation is transformed into plastic deformation. Meanwhile, the mechanical strengths are enhanced due to age hardening effect. CAF is successfully applied to the upper wing skin of the executive jet Gulfstream IV/V, B1B and Hawk bombers, and the commercial A330/340/380 Airbus jets[4]. According to the thermal load, CAF process can be classified as the isothermal creep aging (ICA) forming and nonisothermal creep aging (NICA) forming.

ICA process can easily improve the strength of alloys[5–6]. However, the inferior corrosion resistance is a significant issue for age-hardened Al-Zn-Mg-Cu alloys[7]. To improve the corrosion resistance of Al-Zn-Mg-Cu alloys, ICA treatment based on CAF mechanism has been widely researched[8–10]. The conventional overaging method is often used in ICA process to improve the corrosion resistance of alloys. However, the long-term aging reduces the mechanical strength of alloys.

In addition, the strict isothermal process can hardly be implemented in the production of large aluminum alloy components. Therefore, the nonisothermal method is proposed due to its flexible process with high efficiency[11–12]. On this basis, it is considered that the nonisothermal aging method should be coupled with CAF technique. Xu et al[13] studied the creep aging behavior of Al-Cu-Mg alloy at different heating rates and found that the creep deformation at the heating stage

Received date: May 31, 2022
Foundation item: Core Technology Research Project of Foshan City (1920001000412); National Defense Basic Scientific Research Program (JCKY2018205B024)
Corresponding author: Li Xiaoqiang, Ph. D., Professor, Guangdong Key Laboratory for Advanced Metallic Materials Fabrication and Forming, South China University of Technology, Guangzhou 510640, P. R. China, E-mail: lixq@scut.edu.cn

is decreased with increasing the heating rates. In addition, Xu et al[14] focused on the nonisothermal creep deformation behavior of Al-Cu-Mg alloy and found that the creep strain at the heating stage is 22.28%–26.86% of the total creep strain. Currently, NICA process is mainly conducted on Al-Cu series alloys. The researches on Al-Zn-Mg-Cu series alloys treated by NICA are rarely reported.

Notably, the creep rate of the alloy increases exponentially during the heating stage[14]. Liu et al[15] believed that the precipitation process can be completed in the heating stage to realize the aging strengthening of the alloys. It can be seen that the alloy forming and aging hardening can both be achieved in the heating stage of CAF. Therefore, the non-isothermal creep aging behavior of the Al-Zn-Mg-Cu alloy was studied in this research. The effects of heating rate and aging temperature on the microstructure, mechanical properties, and corrosion resistance of Al-Zn-Mg-Cu alloy treated by NICA process were studied, and the precipitation behavior of Al-Zn-Mg-Cu alloy in NICA process was discussed.

1 Experiment

In this research, the rolled Al-Zn-Mg-Cu alloy plate was used, and its chemical composition is shown in Table 1. The specimens with size of 200 mm×100 mm×2 mm were cut along the rolling direction of the plate. Before CAF process, the specimens were treated by solution in the resistance furnace. The specimens were kept at 480 °C for 1 h and then water-quenched immediately. NICA forming tests were also conducted in the resistance furnace. To facilitate rapid sampling, specific molds were used for mechanical loading, as shown in Fig. 1. The screws were tightened at the same position of each test. To ensure that the specimen deformation is within the elastic range of the material, the curvature radius of the mold was selected as 1000 mm.

The peak temperature of NICA process was 160–200 °C, and the heating rate was 10–40 °C/h. The aging time was calculated by the peak temperature, room temperature (25 °C), and heating rate. As for NICA process under heating rate of 10 °C/h and peak temperature of 160 °C, the aging time was (160 − 25)/10=13.5 h. The mold and the specimen were together heated from room temperature to the peak temperature at a certain heating rate, and then the specimen was immediately removed and cooled to room temperature. Air cooling was adopted in this research, which was closer to the actual production conditions. In addition, the peak-aging without stress and the common ICA process were also conducted. In ICA process, the mold and the specimen were heated from room temperature to 120 °C at heating rate of 5 °C/min and held for 24 h[16]. The specimens for peak-aging process without stress were heated to 120 °C and kept for 24 h[7].

Table 1 Chemical composition of rolled Al-Zn-Mg-Cu alloy plate (wt%)

Zn	Mg	Cu	Mn	Fe	Cr	Si	Ti	Al
5.95	2.06	1.46	0.26	0.12	0.13	0.05	0.01	Bal.

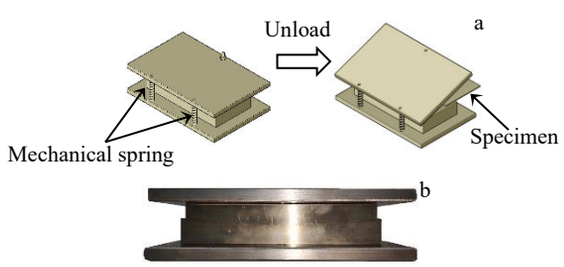

Fig.1 Schematic diagram (a) and appearance (b) of CAF die and specimen

At the end of NICA process, the specimens were inevitably recovered after the external force was removed. The springback η could be calculated by Eq.(1)[17], as follows:

$$\eta = \frac{d_{\max} - d}{d_{\max}} \times 100\% \quad (1)$$

where $d_{\max}$ is the maximum vertical distance between the initial specimen and the surface of the forming tool, and d is the maximum vertical distance between the formed specimen and the initial specimen, as shown in Fig.2.

Vickers hardness was measured by the micro-Vickers hardness tester (HVS-1000). The tensile tests were performed by the CMT5105 electronic universal testing machine at tensile speed of 2 mm/min. The methods for measurement and calculation of the springback were based on the ones in Ref.[18].

Intergranular corrosion (IGC) and exfoliation corrosion (EXCO) tests were conducted according to ASTM G110-92 and ASTM G34-01 standards, respectively. The specimens were cut into small pieces of 10 mm×15 mm×2 mm. In IGC tests, the specimens were corroded in a deionized aqueous solution of 57 g/L NaCl+10 mL/L H_2O_2. The experiment temperature was controlled at 35±1 °C for 6 h. The corrosion solution for EXCO tests was composed of 4 mol/L sodium chloride, 0.5 mol/L potassium nitrate, and 0.1 mol/L nitric acid. The specimens were immersed in the corrosion solution at 25±3 °C for 48 h. The corrosion degree was evaluated according to the spalling corrosion rate, which could be classified as no obvious corrosion (N), slight pitting (P), pitting growth (EA), slight surface cracking (EB), surface spalling and bubbling (EC), and severe erosion product stripping (ED).

After IGC, the specimens were observed by DMi 5000

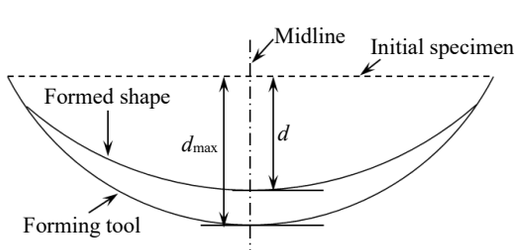

Fig.2 Schematic diagram of springback

metallographic microscope (OM). Scanning electron microscope (SEM, FEI Nova Nano 430) was used to observe EXCO surface of the specimens. The precipitate microstructures in Al-Zn-Mg-Cu alloy were observed by Talos F200X transmission electron microscope (TEM). The specimens were mechanically thinned to 60 μm in diameter and then twinjet electropolished in the solution of 30vol% perchloric acid and 70vol% ethanol at −20 °C and 20 V. The methods for precipitate measurement were based on the ones in Ref.[19–20].

2 Results and Discussion

2.1 Hardness

The hardness of Al-Zn-Mg-Cu alloy can reflect the hardening effect of NICA process on the alloy[21]. Fig.3 shows the hardness of Al-Zn-Mg-Cu alloys after NICA treatments at different peak temperatures and different heating rates. Under a fixed peak temperature, the hardness changes differently with increasing the heating rate. When the peak temperature is 160 °C, the alloy hardness is decreased with increasing the heating rate. When the peak temperature rises to 180 °C, the alloy hardness is rapidly increased and then decreased slowly with increasing the heating rate. When the peak temperature is 200 °C, the alloy hardness is increased with increasing the heating rate. When the heating rate is 20 °C/h and the peak temperature is 180 °C, the maximum hardness of the alloy is 1870.8 MPa, which is slightly lower than the hardness of alloy after peak-aging and still higher than that after ICA process.

Because the hardness variation trend is not monotonous when the peak temperature is 180 °C, the influence of heating rate on the springback and tensile properties of alloy after NICA process with peak temperature of 180 °C need further investigation. In addition, since the highest hardness is achieved at heating rate of 20 °C/h and the peak temperature of 180 °C, the effect of the peak temperature on the springback and tensile properties of the alloy at heating rate of 20 °C/h should also be studied.

2.2 Springback

Fig. 4 shows the springback of Al-Zn-Mg-Cu alloy treated by NICA process at different peak temperatures and heating rates. Fig. 4a shows that the springback is increased gradually with increasing the heating rate. When the heating rate is 10 °C/h, the springback is the lowest of 54.1%. The springback increases to 68.5% when the heating rate increases to 40 °C/h. Fig. 4b shows that the springback is decreased with increasing the peak temperature. When the peak temperature is 160 °C, the springback is 65.42%. As the peak temperature rises to 200 °C, the springback decreases to 56.81%.

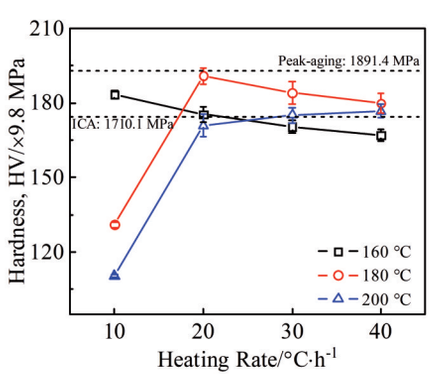

Fig.3 Effect of peak temperature and heating rate on hardness of Al-Zn-Mg-Cu alloy after NICA treatment

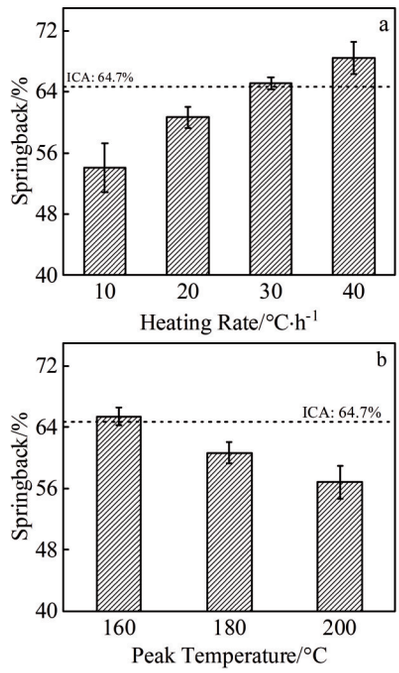

Fig.4 Springback of Al-Zn-Mg-Cu alloy after NICA treatment under different conditions: (a) peak temperature of 180 °C with different heating rates; (b) heating rate of 20 °C/h with different peak temperatures

In the creep aging process, the stress relaxation in the specimen is not complete. Thus, the elastic deformation under initial loading cannot be fully transformed into permanent plastic deformation. After removing the load, the specimen is inevitably recovered. Therefore, the stress relaxation degree of the specimen can directly affect the final springback. The stress relaxation in Al-Zn-Mg-Cu alloy is induced by the dislocation movement under thermal activation, which causes permanent deformation in the alloy[22]. Under the conditions of the same mold and constant peak temperature, the higher the heating rate, the shorter the dislocation movement duration and thereby the less the transformation from elastic deformation to plastic deformation. These phenomena result in the large remaining elastic deformation after aging, i.e., the high springback of alloy after unloading. Under the conditions of the same mold and constant heating rate, the increase in peak temperature accelerates the dislocation movement and provides more time for dislocation movement, thus promoting the transformation from elastic deformation to plastic deformation, reducing the remaining elastic deformation after aging, and finally reducing the springback.

2.3 Tensile properties

Fig. 5 shows the yield strength, tensile strength, and elongation of the Al-Zn-Mg-Cu alloy treated by NICA process at different heating rates and peak temperatures. It can be seen that the variation trend of strength is consistent with that of hardness. As shown in Fig. 5a, when the peak temperature is 180 °C, the yield strength and tensile strength of the alloy are increased firstly and then decreased with increasing the heating rate. Under heating rate of 20 °C/h, as shown in Fig. 5b, the yield strength and tensile strength are also increased firstly and then decreased with increasing the peak temperature. The variation trend of elongation is opposite to that of yield strength or tensile strength. When the heating rate is 20 °C/h and the peak temperature is 180 °C, the yield strength and tensile strength of the alloy reach the maximum values of 546.9 and 580.7 MPa, respectively; the elongation reaches the minimum value of 9.6%.

Table 2 shows the tensile properties of Al-Zn-Mg-Cu alloy after different aging processes. The yield strength and tensile strength of alloy after NICA process (180 °C, 20 °C/h) are close to those after peak-aging treatment and higher than those after ICA treatment. It is worth noting that the aging duration of ICA treatment is approximately 24 h, and the springback of the alloy after aging is 64.7%. However, NICA process duration is approximately 7.8 h, and the springback is only 60.7%, which indicates that the aging time is shortened by 67% and the aging efficiency of NICA process is significantly higher than ICA process.

2.4 Corrosion behavior

2.4.1 IGC tests

Fig.6 and Table 3 show the IGC cross section morphologies and maximum IGC depth of the Al-Zn-Mg-Cu alloy after different aging processes, respectively. The larger the maximum corrosion depth, the worse the corrosion resistance of alloy. It can be seen that the maximum IGC depth is increased with increasing the heating rate. At heating rate of 10 °C/h, the maximum IGC depth is only 41.3 μm; at heating rate of 30 °C/h, the maximum IGC depth increases to 98.9 μm. In addition, with increasing the peak temperature, the maximum IGC depth is decreased. The maximum IGC depth is decreased from 110.0 μm to 39.6 μm with increasing the peak temperature from 160 °C to 200 °C. Besides, the

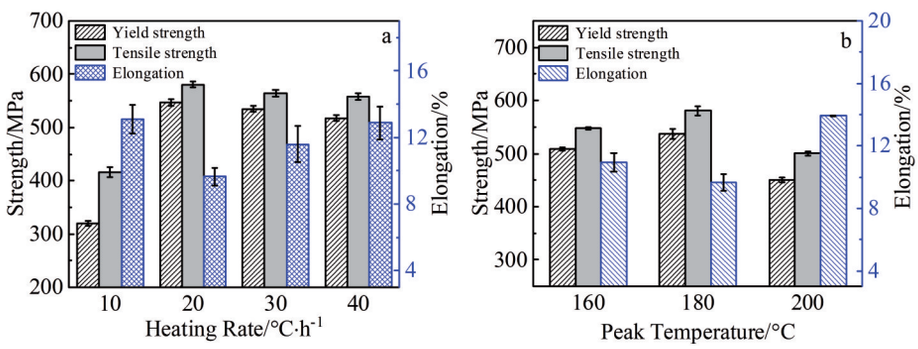

Fig.5 Tensile properties of Al-Zn-Mg-Cu alloy after NICA treatment under different conditions: (a) peak temperature of 180 °C with different heating rates; (b) heating rate of 20 °C/h with different peak temperatures

Table 2 Tensile properties of Al-Zn-Mg-Cu alloy after different aging processes

Aging process	Yield strength/MPa	Tensile strength/MPa	Elongation/%
NICA (180 °C, 20 °C/h)	546.9	580.7	9.6
Peak-aging	540.1	582.6	9.4
ICA	523.2	572.7	14.8

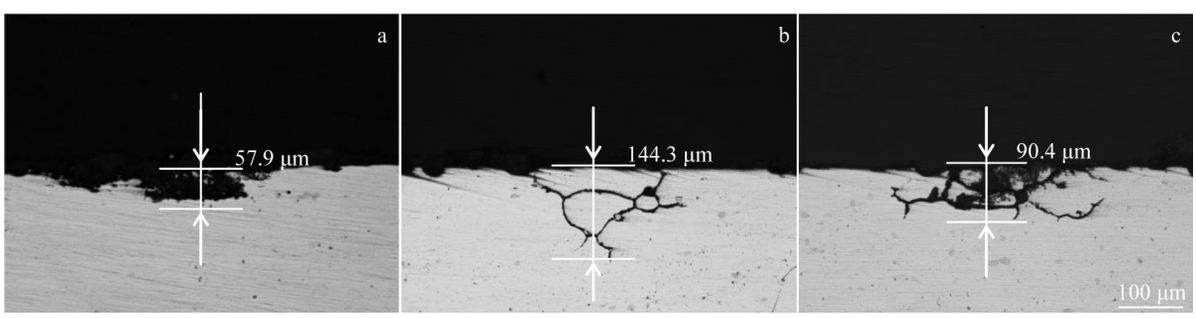

Fig.6 IGC cross section morphologies of Al-Zn-Mg-Cu alloy after different aging processes: (a) NICA (180 °C, 20 °C/h) process, (b) peak-aging process, and (c) ICA process

Table 3 Maximum IGC depth of Al-Zn-Mg-Cu alloy after different aging processes

Aging process	Maximum IGC depth/μm
NICA (180 °C, 10 °C/h)	41.3
NICA (180 °C, 20 °C/h)	57.9
NICA (180 °C, 30 °C/h)	98.9
NICA (160 °C, 20 °C/h)	111.0
NICA (200 °C, 20 °C/h)	39.6
Peak-aging	144.3
ICA	90.4

maximum IGC depth of Al-Zn-Mg-Cu alloy treated by NICA (180 °C, 20 °C/h) process is lower than that treated by ICA and peak-aging, indicating the optimal corrosion resistance.

2.4.2 EXCO tests

Fig. 7 and Table 4 show EXCO surface morphologies and the corrosion degrees of Al-Zn-Mg-Cu alloy treated by different aging conditions after EXCO tests. The EXCO change law is consistent with IGC variation trend. At the heating rate of 10 °C/h, after EXCO for 48 h, the corrosion degree of alloy is PB; when the heating rate increases to 30 °C/h, the corrosion degree of alloy is EC, indicating that the corrosion is increased with increasing the heating rate. When the peak temperature increases from 160 °C to 200 °C, the corrosion degree changes from ED to PB, suggesting that the corrosion is decreased with increasing the peak temperature. In addition, the corrosion degree of the alloy treated by NICA (180 °C, 20 °C/h) process is less severe than that treated by ICA and peak-aging processes.

2.5 Microstructure

The precipitation sequence in Al-Zn-Mg-Cu alloy during nonisothermal aging process is as follows: supersaturated solid solution→GP zones→ η' phase→ η phase[23]. Since the precipitation sequence cannot be changed by the introduction of stress[24], the precipitation sequence of the Al-Zn-Mg-Cu alloy during NICA process does not change, either.

2.5.1 Intragranular precipitates

Fig. 8 shows TEM bright field images along $[110]_{Al}$ direction of the Al-Zn-Mg-Cu alloy after different NICA treatments. Table 5 shows the results of precipitate size (radius) and content. At the heating rate of 10 °C/h and peak temperature of 180 °C, the precipitates with average radius of 8.8 nm and content of 2.05vol% are sparsely distributed in the alloy. When the heating rate increases to 20 ° C/h, the precipitate distribution in the alloy becomes denser; the average radius decreases to approximately 3.6 nm; the content of precipitate increases slightly to approximately 2.33vol% . When the heating rate further increases to 30 ° C/h, the precipitate size decreases slightly to 3.1 nm, and the precipitate content decreases sharply to approximately 1.79vol% . As a result, at peak temperature of 180 °C, the precipitate size is decreased with increasing the heating rate, whereas the precipitate content is firstly increased and then decreased.

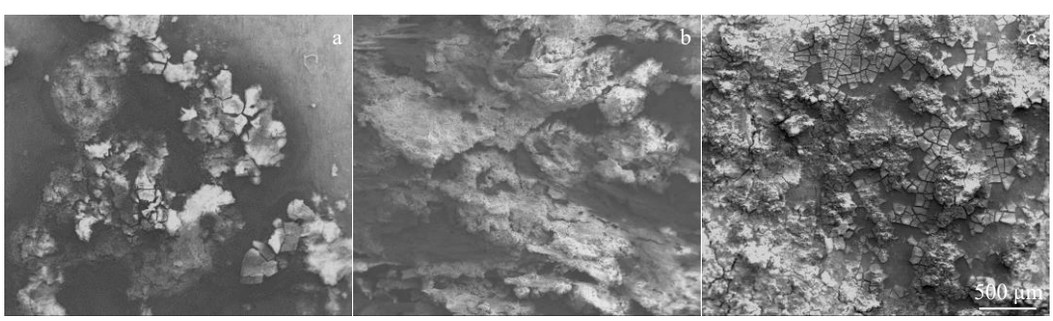

Fig.7 EXCO surface morphologies of Al-Zn-Mg-Cu alloy treated by different aging processes: (a) NICA (180 °C, 20 °C/h) process, (b) peak-aging process, and (c) ICA process

Under the condition of fixed heating rate of 20 °C/h, when the peak temperature is 160 ° C, the precipitate size is approximately 3.3 nm and the precipitate content is approximately 1.27vol% . The precipitate size and content are both increased with increasing the peak temperature to 180 ° C. When the peak temperature gradually increases to 200 °C, the precipitate size increases significantly to 6.2 nm, and the precipitate content decreases slightly to 2.26vol% . Therefore, when the heating rate is constant at 20 °C/h, with increasing the peak temperature, the precipitate size is increased while the precipitate content is increased firstly and then decreased.

To further determine the type of precipitates, high-

Table 4 Exfoliation corrosion degrees of Al-Zn-Mg-Cu alloy after different aging conditions

Aging process	EXCO duration/h			
	1	8	24	48
NICA (180 °C, 10 °C/h)	N	N	P	P
NICA (180 °C, 20 °C/h)	N	N	P	EA
NICA (180 °C, 30 °C/h)	N	P	EA	EC
NICA (160 °C, 20 °C/h)	N	P	EB	ED
NICA (200 °C, 20 °C/h)	N	N	P	P
Peak-aging	N	P	EB	ED
ICA	N	N	P	EB

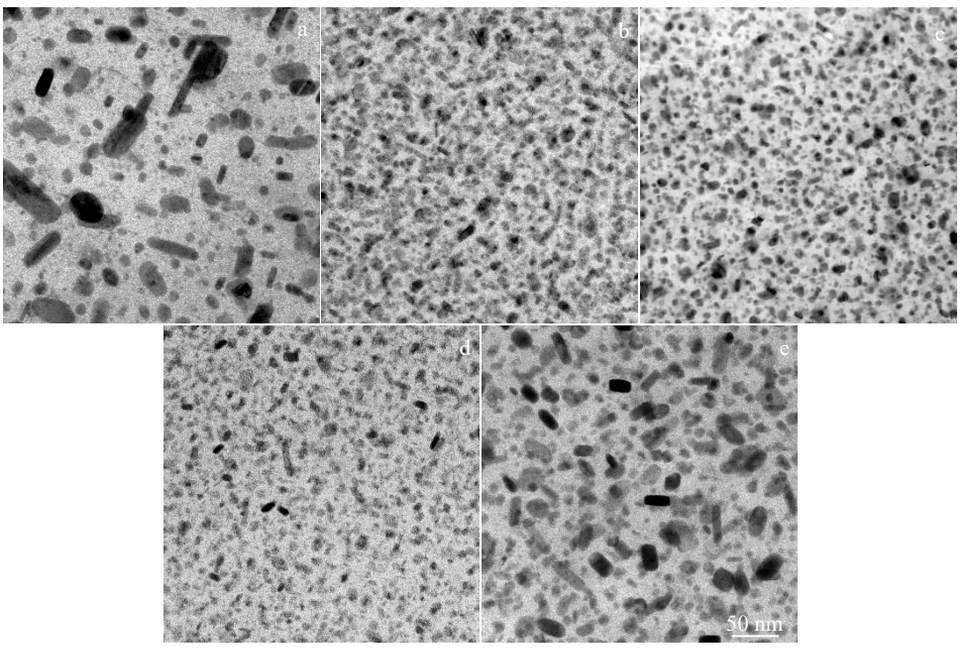

Fig.8 TEM bright field images along $[110]_{Al}$ direction of Al-Zn-Mg-Cu alloy treated by different NICA processes: (a) 180 °C, 10 °C/h; (b) 180 °C, 20 °C/h; (c) 180 °C, 30 °C/h; (d) 160 °C, 20 °C/h; (e) 200 °C, 20 °C/h

Table 5 Average radius and content of precipitates in Al-Zn-Mg-Cu alloy after different NICA treatments

Aging process	Average radius/nm	Content/vol%
NICA (180 °C, 10 °C/h)	8.8	2.05
NICA (180 °C, 20 °C/h)	3.6	2.33
NICA (180 °C, 30 °C/h)	3.1	1.79
NICA (160 °C, 20 °C/h)	3.3	1.27
NICA (200 °C, 20 °C/h)	6.2	2.26

resolution TEM (HRTEM) was used to observe the local area in Fig. 8, and the characteristic regions of precipitates were analyzed by fast Fourier transform (FFT) method. Chung et al[25] also used this method to identify the types of aging precipitates in Al-Zn-Mg-Cu series aluminum alloys.

Fig. 9 shows HRTEM images of the precipitates in Al-Zn-Mg-Cu alloy after different NICA processes and FFT patterns corresponding to the marked regions.

According to Fig. 9a, $9a_1$, and $9a_2$, under the conditions of peak temperature of 180 °C and heating rate of 10 °C/h, only aluminum matrix can be observed in region A and the η phase[25] exists in region B. Therefore, only the η precipitate phase (represented by blue arrow in Fig. 9) appears in Al-Zn-Mg-Cu alloy after NICA (180 °C, 10 °C/h) process. As shown in Fig. 9b and $9b_1-9b_4$, the GP zone (represented by yellow arrow in Fig. 9), η phase, and η' phase (represented by white arrow in Fig. 9) appear in Al-Zn-Mg-Cu alloy after NICA (180 °C, 20 °C/h) process. It can be seen that the η' phase is the main precipitate phase, and GP zone and η phase only account for a small proportion. As shown in Fig. 9c and $9c_1-9c_4$, the precipitates in alloy after NICA (180 °C, 30 °C/h) treatment include the η' phase, which is proved by FFT pattern at $1/3\{220\}_{Al}$ and $2/3\{220\}_{Al}$[26], as well as the GP zone and η' phase. It can be seen that GP zone and η' phase are the main precipitates in this case, and η phase only accounts for a small proportion. As shown in Fig.9d and $9d_1-9d_3$, after NICA (160 °C, 20 °C/h) treatment, the precipitates in the Al-Zn-Mg-Cu alloy are mainly η' phase and GP zone. η phase cannot be observed. As shown in Fig. 9e, $9e_1$, and $9e_2$, only η phase can be found, indicating that after NICA (200 °C, 20 °C/h) treatment, the main precipitates in the alloy are η phase.

The change in peak temperature can roughly reflect the microstructure evolution during NICA process. At the initial stage of NICA, due to the low aging temperature, the precipitates mainly nucleate at favorable positions with high energy in the supersaturated solid solution, resulting in the early precipitation of GP zone. With increasing the aging temperature, the nucleation driving force of precipitates is increased, and the nucleation occurs at the area with relatively low energy. At the same time, the as-nucleated GP zone grows and changes into η' phase. Therefore, the main precipitates in the alloy gradually become GP zone and η' phase when the temperature increases to 160 °C. When the aging temperature continues to increase, the nucleation sites further increase, new precipitates continue to appear, the existing GP zone and η' phase grow, and the precipitation in the alloy becomes more sufficient. At this time, GP zone mainly changes into η' phase, which increases the content of η' phase. However, only a small amount of η' phase can change into η phase due to the restriction of peak-aging temperature. Therefore, GP zone, η' phase, and η phase all exist in the alloy, and the content of η' phase is the highest when the temperature reaches the peak-aging temperature of 180 °C. When the aging temperature further increases to 200 °C, a large amount of η' phase is

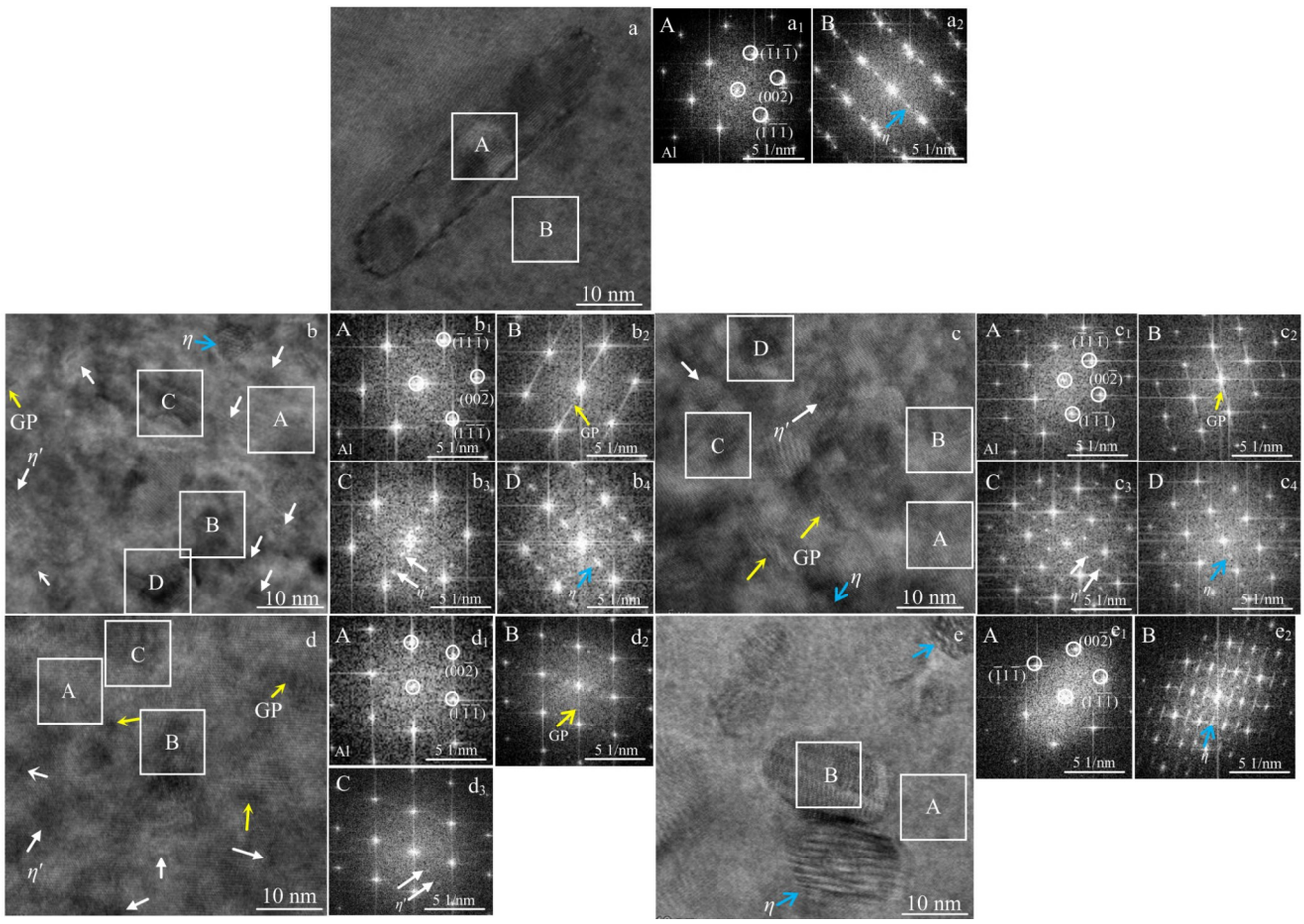

Fig.9 HRTEM images (a–e) and corresponding FFT patterns (a_1–a_2, b_1–b_4, c_1–c_4, d_1–d_3, e_1–e_2) of precipitates in Al-Zn-Mg-Cu alloy after different NICA processes: (a, a_1–a_2) 180 °C, 10 °C/h; (b, b_1–b_4) 180 °C, 20 °C/h; (c, c_1–c_4) 180 °C, 30 °C/h; (d, d_1–d_3) 160 °C, 20 °C/h; (e, e_1–e_2) 200 °C, 20 °C/h

coarsened and transformed into η phase, and the precipitates of large particles are attached to the precipitates of surrounding small particles, reducing the number of precipitates and increasing the content of η phase in the alloy.

2.5.2 Intragranular precipitates related to mechanical properties

Aging strengthening is the most effective strengthening mechanism for the Al-Zn-Mg-Cu alloy[27]. The precipitated particles affect the strength of alloy by hindering the dislocation movement. Dislocation motion must cut through or bypass precipitated particles. Therefore, the aging strengthening mechanism can be classified as the shear strengthening mechanism and the Orowan strengthening mechanism. For the small precipitates collocated or semi-collocated with the aluminum matrix, such as GP zone and η' phase in the early aging stage, the precipitated particles are cut through by the dislocation movement, indicating the shear strengthening mechanism. The shear strengthening effect of precipitates $\Delta\sigma_A$ can be expressed by Eq.(2)[28], as follows:

$$\Delta\sigma_A = C_1 f^m r^n \quad (2)$$

where C_1, m, and n are constants; f is the volume fraction of the precipitates; r is the precipitate radius.

With the aging process proceeding, the precipitates gradually become incoherent with the matrix, and the dislocations tend to bypass the particles, suggesting the Orowan strengthening mechanism. The yield strength $\Delta\sigma_B$ caused by Orowan strengthening mechanism can be expressed by Eq.(3)[29], as follows:

$$\Delta\sigma_B = C_2 f^{\frac{1}{2}} r^{-1} \quad (3)$$

where C_2 is a constant.

The strength of Al-Zn-Mg-Cu alloy after aging depends on the competition result or synergy effect between the two strengthening mechanisms. It is generally believed that the shear strengthening mechanism has a better effect on strengthening than the Orowan strengthening mechanism[27]. Therefore, according to Eq.(2) and Eq.(3), the ideal condition of aging strengthening is that the volume fraction of precipitates is as large as possible; the precipitate size is moderate for dislocations to cut through the precipitates instead of bypassing them.

At the heating rate of 10 °C/h, it can be seen that the main precipitates in the alloy are η phase with a sparse distribution. At this time, the Orowan strengthening mechanism plays the dominant role, and the alloy strength is not that high due to

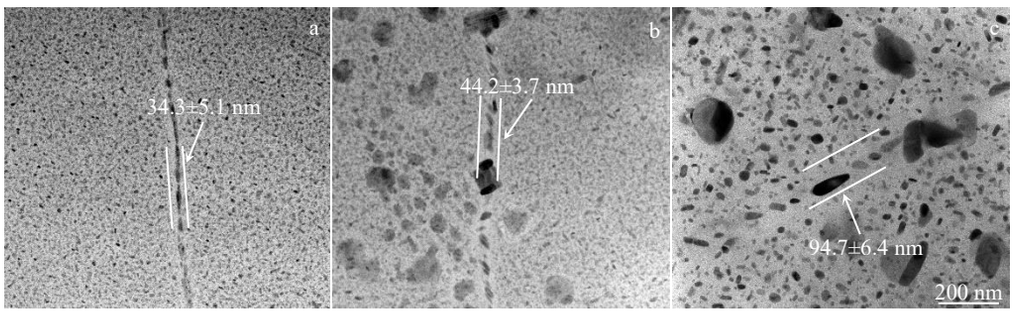

Fig.10 TEM morphologies of grain boundaries in Al-Zn-Mg-Cu alloys after different NICA processes: (a) 160 °C, 20 °C/h; (b) 180 °C, 20 °C/h; (c) 180 °C, 10 °C/h

the relatively weak strengthening effect. When the heating rate increases to 20 °C/h, the volume fraction of precipitate in the alloy increases, and the main precipitates are η' phase accompanied by a small amount of GP zone and η phase, indicating that the shear strengthening mechanism is the dominate strengthening mechanism accompanied by the synergistic effect of the Orowan strengthening mechanism. This result increases the alloy strength dramatically. When the heating rate further increases to 30 °C/h, the precipitates in the alloy are mainly GP zone and η' phase with a small amount of η phase. Thus, the strengthening mechanism is mainly the shear strengthening mechanism accompanied by the synergistic effect of the Orowan strengthening mechanism. However, the precipitate size and content are smaller at the heating rate of 30 ° C/h, which conversely hinders the enhancement in alloy strength. Therefore, the alloy strength at the heating rate of 30 °C/h is relatively low. Briefly, the high strength of Al-Zn-Mg-Cu alloy after NICA (180 °C, 20 °C/h) process is caused by the high volume fraction and appropriate size of precipitates rather than the change in peak temperature and heating rate.

2.5.3 Microstructure related to corrosion resistance

In the Al-Zn-Mg-Cu alloy, the grain boundary precipitates (GBPs) and precipitate-free zones (PFZs) have direct influence on the corrosion resistance of the alloy[30–31]. Fig. 10 shows TEM morphologies of the grain boundaries in Al-Zn-Mg-Cu alloy treated by different NICA processes. As shown in Fig. 10a, after NICA (160 °C, 20 °C/h) treatment, partial GBPs in the alloy are continuous, and others present the chain discontinuous state. The width of PFZ is approximately 34.3± 5.1 nm. Because the dissolution potential of GBPs is lower than the pitting potential of the matrix, GBPs are preferentially dissolved as anodes under corrosion conditions. When GBPs are continuously distributed in the alloy, they easily form the anodic corrosion channels and accelerate the corrosion process. Therefore, the inferior corrosion resistance of Al-Zn-Mg-Cu alloy is caused by the continuous GBPs, which act as the corrosion path. When the peak temperature increases to 180 °C, as shown in Fig. 10b, the distribution of GBPs is obviously discontinuous, the size of GBPs increases, and the width of PFZ increases to 44.2±3.7 nm, which improves the corrosion resistance of the alloy. This is because the increase in peak temperature promotes the dislocation movement, thus increasing the diffusion rate of solute atoms at grain boundaries, promoting the growth of some GBPs, and breaking the GBP continuity. In addition, the growth of precipitates consumes the solute atoms at the grain boundary, resulting in the expansion of PFZ. When the heating rate decreases from 20 °C/h to 10 °C/h, as shown in Fig. 10c, the size of GBPs increases, and the PFZ becomes wider of 94.7± 6.4 nm in width, indicating that the alloy has good corrosion resistance. Under the same peak temperature, the lower the heating rate, the longer the aging duration of alloy and the more sufficient the GBP growth and coarsening.

3 Conclusions

1) After nonisothermal creep aging (NICA) treatment at heating rate of 20 °C/h and peak temperature of 180 °C, the main precipitates of the Al-Zn-Mg-Cu alloy are dense η' phase. The hardness of the alloy after NICA (180 °C, 20 °C/h) process is 1870.8 MPa, the yield strength is 546.9 MPa, and the tensile strength is 580.7 MPa. The tensile properties of the Al-Zn-Mg-Cu alloy after NICA (180 °C, 20 °C/h) process are better than those after the isothermal creep aging (ICA) - treated alloy. In addition, the springback of NICA-treated alloy is 60.7%, which is lower than that of the ICA-treated alloy.

2) The decrease in heating rate and the increase in peak temperature can improve the intergranular corrosion resistance and exfoliation corrosion resistance of Al-Zn-Mg-Cu alloy. After NICA treatment at heating rate of 20 ° C/h and peak temperature of 180 ° C, the grain boundary precipitates are discontinuous, and PFZ width is approximately 44.2 nm, which results in the improved corrosion resistance of the alloy.

3) NICA process can improve the corrosion resistance of the alloy without degrading the mechanical strength. Besides, NICA process shows higher aging efficiency, which is suitable for practical production.

References

1 Williams J C, Starke E A. *Acta Materialia*[J], 2003, 51(19): 5775

2 Dursun T, Soutis C. *Materials & Design*[J], 2014, 56: 862

3 Yang D L, Liang M, Miao J J *et al*. *Journal of Physics*

Conference Series[J], 2020, 1622: 12 095
4 José I D, Roberto C, Ferreira F F *et al*. *Materials Research*[J], 2012, 15(4): 596
5 Jeshvaghani R A, Shahverdi H R, Hadavi S. *Materials Science and Engineering A*[J], 2012, 552: 172
6 Jeshvaghani R A, Emami M, Shahverdi H R *et al*. *Materials Science and Engineering A*[J], 2011, 528(29–30): 8795
7 Zhang Guohui, Yang Xiubo, Huang Leiping *et al*. *Rare Metal Materials and Engineering*[J], 2018, 47(11): 3393 (in Chinese)
8 Xu L Z, Zhan L H, Xu Y Q *et al*. *Journal of Materials Processing Technology*[J], 2021, 293(17–18): 117 089
9 Wang Q, Zhang L H, Xu Y Q *et al*. *Transactions of Nonferrous Metals Society of China*[J], 2020, 30(10): 2599
10 Zhang J, Wang Y, Deng Y L *et al*. *Materials Science and Engineering A*[J], 2016, 664: 126
11 Jiang F L, Zhang H. *Journal of Materials Science*[J], 2018, 53(4): 2830
12 Myriam N, Alexis D. *Acta Materialia*[J], 2003, 51(20): 6077
13 Xu Y Q, Zhan L H, Ma Z Y *et al*. *Materials Science and Engineering A*[J], 2017, 688: 488
14 Xu Y Q, Zhan L H, Huang M H *et al*. *Journal of Materials Processing Technology*[J], 2018, 255: 26
15 Liu Y, Jiang D M, Li B Q *et al*. *Materials & Design*[J], 2014, 60: 116
16 Lei C, Li H, Fu J *et al*. *Materials Characterization*[J], 2018, 144: 431
17 Brandão F M, Delijaicov S, Bortolussi R. *International Journal of Advanced Manufacturing Technology*[J], 2017, 91: 3273
18 Ho K C, Lin J, Dean T A. *International Journal of Plasticity*[J], 2004, 20(4–5): 733
19 Dumont M, Lefebvre W, Doisneau-Cottignies B *et al*. *Acta Materialia*[J], 2005, 53(10): 2881
20 Li K, Idrissi H, Sha G *et al*. *Materials Characterization*[J], 2016, 118: 352
21 Jeshvaghani R A, Shahverdi H R, Hadavi S M M. *Materials Science and Engineering A*[J], 2012, 552: 172
22 Zhou L C, Cheng J L, Wang W L *et al*. *Rare Metal Materials and Engineering*[J], 2021, 50(11): 4095
23 Gang S, Cerezo A. *Acta Materialia*[J], 2004, 52(15): 4503
24 Lin Y C, Jiang Y Q, Chen X M *et al*. *Materials Science and Engineering A*[J], 2013, 588: 347
25 Chung T F, Yang Y L, Shiojiri M *et al*. *Acta Materialia*[J], 2019, 174: 351
26 Stiller K, Warren P J, Hansen V *et al*. *Materials Science and Engineering A*[J], 1999, 270(1): 55
27 Jia Y D, Cao F Y, Ning Z L *et al*. *Materials & Design*[J], 2012, 40: 536
28 Shercliff H R, Ashby M F. *Acta Metallurgica et Materialia*[J], 1990, 38(10): 1789
29 Thevenet D, Mliha-Touati M, Zeghloul A. *Materials Science and Engineering A*[J], 1999, 266(1–2): 175
30 Ren J, Wang R C, Peng C Q *et al*. *Materials Characterization*[J], 2020, 162: 110 190
31 Altenbach C, Schnatterer C, Mercado U A *et al*. *Journal of Alloys and Compounds*[J], 2020, 817: 152 722

非等温蠕变时效对 Al-Zn-Mg-Cu 合金力学性能和耐腐蚀性能的影响

王令姣[1,2]，李小强[1,2]，潘存良[1,2]，朱德智[1,2]，屈盛官[1,2]，黄　遐[3]
(1. 华南理工大学 广东省金属新材料制备与成形重点实验室，广东 广州 510640)
(2. 华南理工大学 国家金属材料近净成形工程技术研究中心，广东 广州 510640)
(3. 中国航空制造技术研究院，北京 100024)

摘　要：研究了非等温蠕变时效处理中升温速率和峰值温度对 Al-Zn-Mg-Cu 合金回弹性能、力学性能和耐腐蚀性能的影响。通过透射电镜分析了合金的析出行为和时效强化机理。结果表明：随着加热速率的降低和峰值温度的升高，合金的回弹率降低；晶内析出相的尺寸增大，而体积分数先增大后减小；晶界析出相逐渐变得不连续，无析出区扩大。经非等温蠕变时效（20 ℃/h，180 ℃）处理后的合金主要析出相为致密的 η'相，晶界析出相不连续，无析出区的宽度约为44.2 nm。非等温蠕变时效（20 ℃/h，180 ℃）处理的合金力学性能和耐腐蚀性能均优于常见的等温蠕变时效（120 ℃，24 h）处理的合金，并且时效时间缩短了 67%。

关键词：Al-Zn-Mg-Cu 合金；非等温蠕变时效；析出相；力学性能；耐腐蚀性能

作者简介：王令姣，女，1997 年生，硕士，华南理工大学广东省金属新材料制备与成形重点实验室，广东 广州 510640，E-mail：2470921775@qq.com